The Uniqueness of Inversion Solutions of the Elliptic Cone Model for Halo Coronal Mass Ejections

X. P. Zhao
W. W. Hansen Experimental Physics Laboratory, Stanford University, USA

— 2006 AGU Fall Meeting —

December 11 – 15, 2006, San Francisco

1. Introduction

• The magnetic configuration of CMEs is supposed to be curved flux ropes with two ends anchored on the solar surface. The curved ropes can be approximated as 3-D elliptic cone-like structure. Halo CMEs are believed to be formed by the Thompson scattering of the 3-D elliptic cone-like shells of CME plasma located far from solar lomb, and the shape of the halos may be modelled by the projection of the 3-D elliptic base of cones on the plane of the sky (POS).

• Some cone-like models have been suggested to be used to invert the real propagation direction, speed, and the angular width of the 3-D cone-like CME plasma from observed 2-D elliptic halos:

Circular cone	Zhao et al., 2002;	Michalek et al., 2003
	Xie et al., 2004;	Xue et al., 2005
Elliptic cone	Zhao, 2004;	Cremades & Bothmer, 2004
Ice Cream cone	Zhao, 2005	

• The circular cone model can be used in very limited cases, though its inversion solution may be unique; the elliptic cone model may be valid for most of halos, but the inversion solution obtained using the methods of Zhao (2004) and Cremades & Bothmer (2004) are not unique.

• Issues to be discussed in the poster:

a. Classication of elliptic halo CMEs

b. The elliptic cone model and its unique inversion solution

c. Validity of various cone-like models

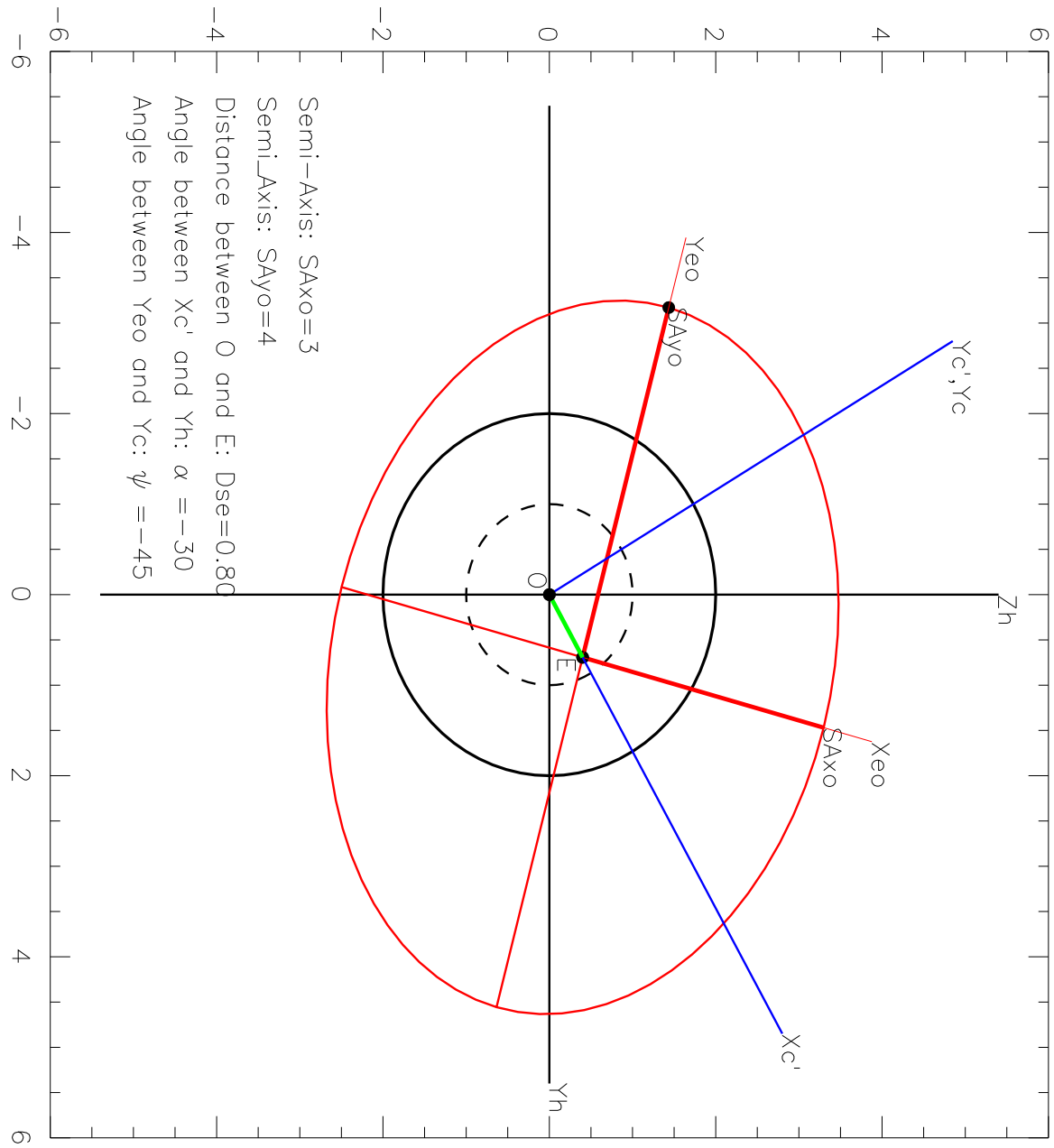

Figure 1. Definition of halo parameters for characterizing elliptic halo CMEs: SA_{xo}, SA_{yo}, ψ, D_{se}, α. Here X_c' and Y_c' (Y_c) are, respectively, aligned with and perpendicular to the distance from the solar disk center to the halo center, D_{se} (the green line).

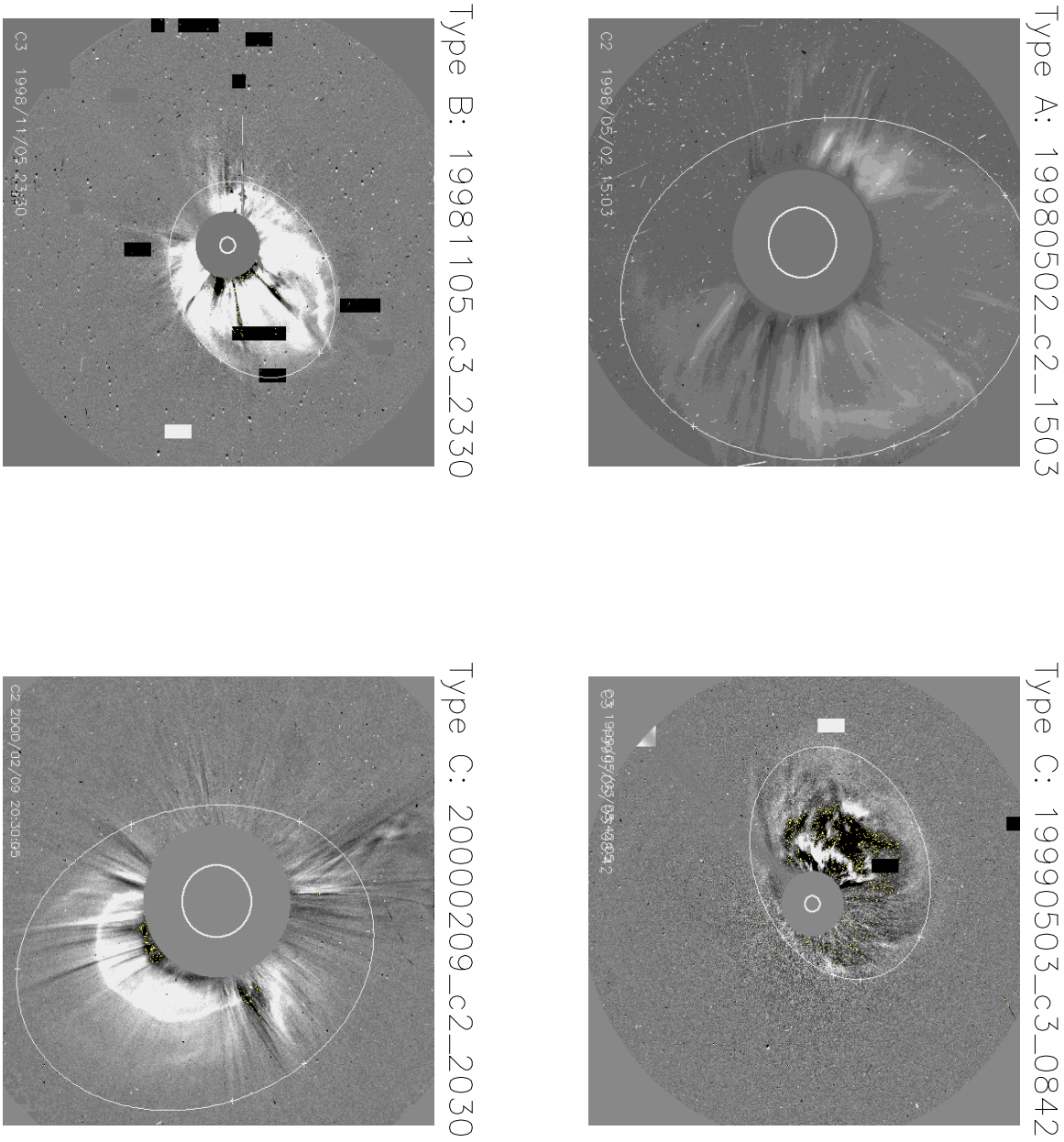

Figure 2. Three types of observed halo CMEs (Courtesy of Hebe Cremades)

2. Description and classification of observed elliptic halos

• Figure 1 shows definition of five halo parameters for characterizing the shape, orientation and location of observed elliptic halos on the plane of the sky ($Y_h Z_h$): (SA_{xo}, SA_{yo}), ψ, (D_{se}, α). Here axes Y_h and Z_h are the west and north axes of the Heliocentric Solar Ecliptic coordinate system with X_h pointed to the Earth. By using halo parameters SA_{xo}, SA_{yo}, ψ, and D_{se} the observed elliptic halo in the plane of $X_c' Y_c'$ (See Figure 1 for the definition of X_c' and Y_c') can be expressed

$$\begin{bmatrix} x_c' \\ y_c' \end{bmatrix} = \begin{bmatrix} \cos\psi & \sin\psi \\ -\sin\psi & \cos\psi \end{bmatrix} \begin{bmatrix} x_{eo} \\ y_{eo} \end{bmatrix} + \begin{bmatrix} D_{se} \\ 0 \end{bmatrix} \tag{1}$$

where

$$\begin{bmatrix} x_{eo} \\ y_{eo} \end{bmatrix} = \begin{bmatrix} SA_{xo} \sin\delta o \\ SA_{yo} \cos\delta o \end{bmatrix} \tag{2}$$

The symbol δo in Eq. (2) is the angle relative to Y_c' or Y_c, and changes along the rim of ellipses from 0° to 360°.

• Figure 2 displays three types of observed elliptic halo CMEs

Type A: $SA_{xo}$is the semi-minor axis and aligned with D_{se}, i.e., $\psi = 0$.

Type B: $SA_{xo}$is the semi-major axis and aligned with D_{se}, i.e., $\psi = 0$.

Type C: $SA_{xo}$is one of semi axes, but not aligned with D_{se}, i.e., $\psi \neq 0$.

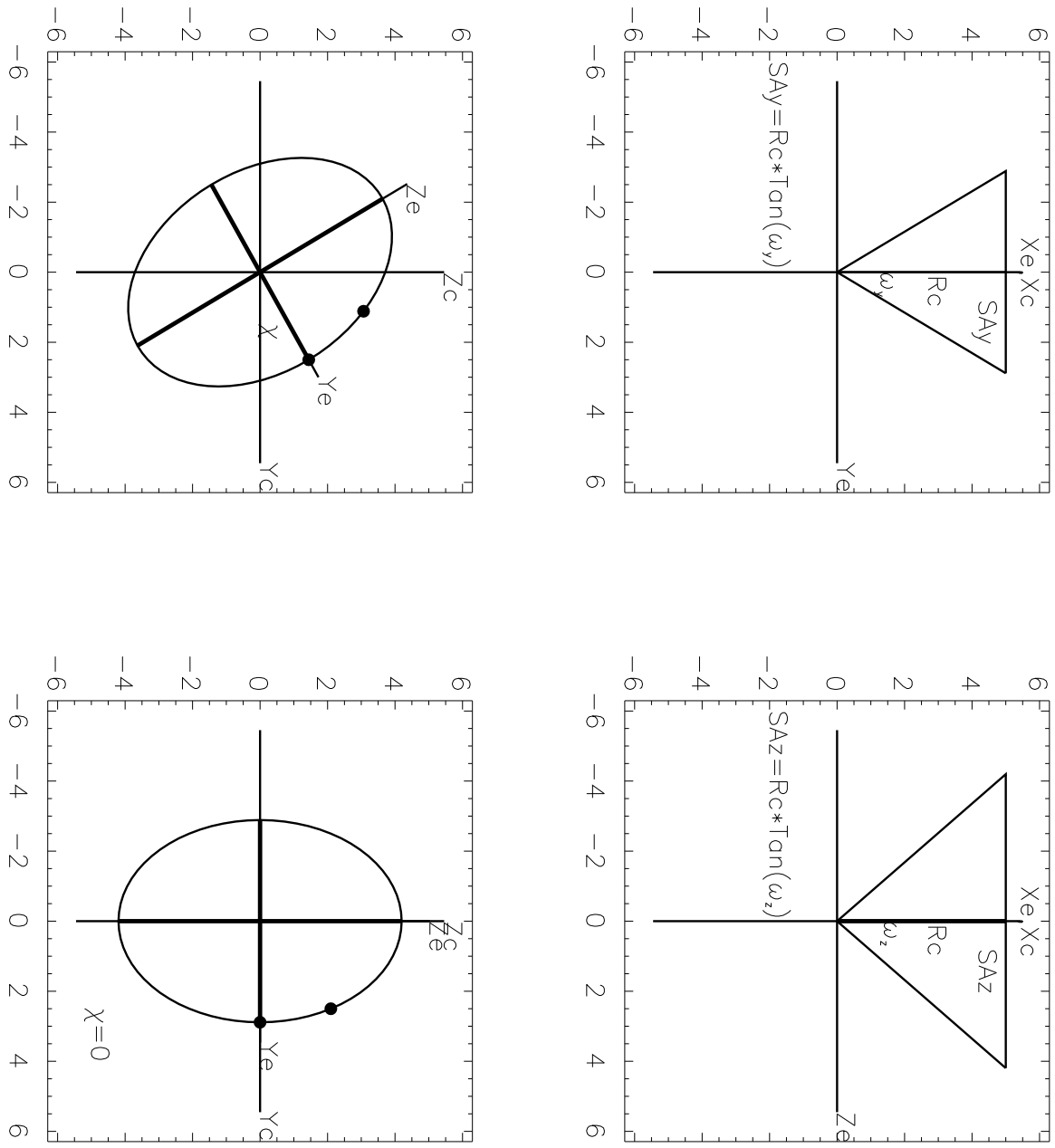

Figure 3. The definition of elliptic cone parameters R_c, ω_y, ω_z, and χ that characterize the distance between apex and base of a cone, and the two semi-axes and orientation of the elliptic base of the cone in the $X_cY_cZ_c$ coordinate system.

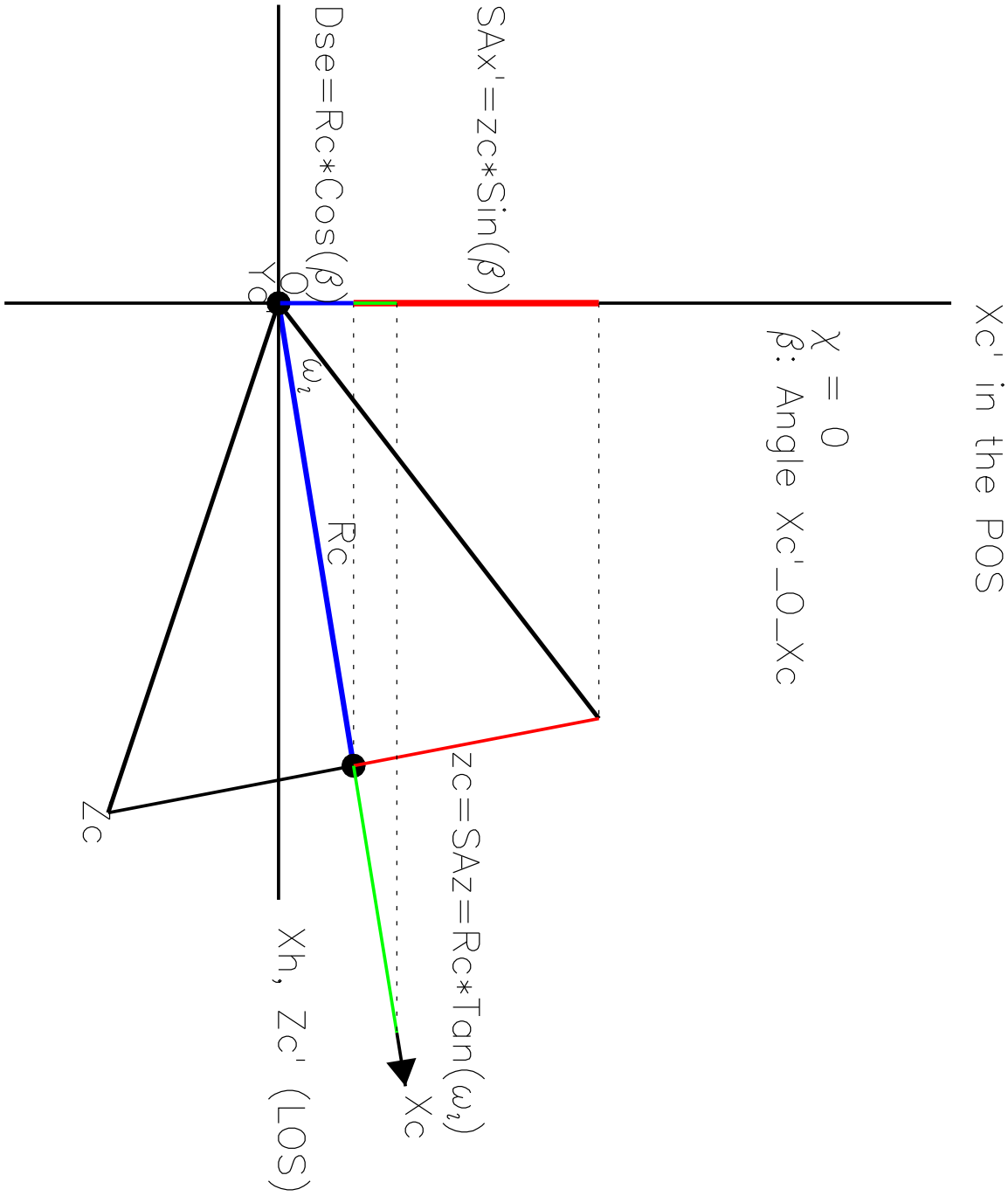

Figure 4. Definitions of the axes X_c (β, α), Y_c, Z_c and X'_c, Y'_c, Z'_c, and the projection of R_c and SA_z on the plane of the sky.

3. The elliptic cone model

Figure 3 shows the definition of elliptic cone parameters R_c, ω_y, ω_z, and χ that characterize 3-D elliptic cone shells in the $X_cY_cZ_c$ coordinate systems. Figure 4 shows the central axis direction X_c of elliptic cones in the $X_hY_hZ_h$ coordinate system and its projection X_c' onto the plane of the sky. The direction of the central axis of cones in $X_hY_hZ_h$system are often expressed using another two elliptic cone parameters, i.e., the latitude λ and longitude ϕ with respect to the eliptic plane (X_hY_h) and the line of sight (X_h axis). However, it is the latitude β and longitude α relative to the plane of the sky (Y_hZ_h) and the local west direction (Y_h axis) that directly determine the projection of the base of cones onto the plane of the sky. The relationship between (β, α) and (λ, ϕ) is (See Figure 5)

$$\left\{ \begin{array}{lcl} \sin\lambda & = & \cos\beta\ \sin\ \alpha \\ \tan\phi & = & \cos\alpha/\tan\beta \end{array} \right\} \left\{ \begin{array}{lcl} \sin\beta & = & \cos\lambda\ \cos\ \phi \\ \tan\alpha & = & \tan\lambda\,/\sin\phi \end{array} \right\} \tag{3}$$

Given a set of R_c, ω_y, ω_z, χ, β and α, halo CMEs in the plane $X_c'Y_c'$ can be produced by the transformation of the rim of elliptic cone bases (x_e, y_e, z_e) from coordinate systems $X_eY_eZ_e$ through $X_cY_cZ_c$ to $X_c'Y_c'Z_c'$.

$$\begin{bmatrix} x_c' \\ y_c' \\ z_c' \end{bmatrix} = \begin{bmatrix} \cos\beta & \sin\beta\sin\chi & -\sin\beta\cos\chi \\ 0 & \cos\chi & \sin\chi \\ \sin\beta & -\cos\beta\sin\chi & \cos\beta\cos\chi \end{bmatrix} \begin{bmatrix} x_e \\ y_e \\ z_e \end{bmatrix} \tag{4}$$

$$\begin{bmatrix} x_e \\ y_e \\ z_e \end{bmatrix} = \begin{bmatrix} R_c \\ R_c\tan\omega_y\cos\delta \\ R_c\tan\omega_z\sin\delta \end{bmatrix} \tag{5}$$

where δ is the angle relative to the axis Y_c, and increase from 0° to 360° along the rim of the base. It is noted that both δo in Eq. (2) and δ here start from Y_c axis.

The halos in the plane $YhZh$ can be obtained

$$\begin{bmatrix} y_h \\ z_h \end{bmatrix} = \begin{bmatrix} \cos\alpha & \sin\alpha \\ -\sin\alpha & \cos\alpha \end{bmatrix} \begin{bmatrix} x'_c \\ y'_c \end{bmatrix} \tag{6}$$

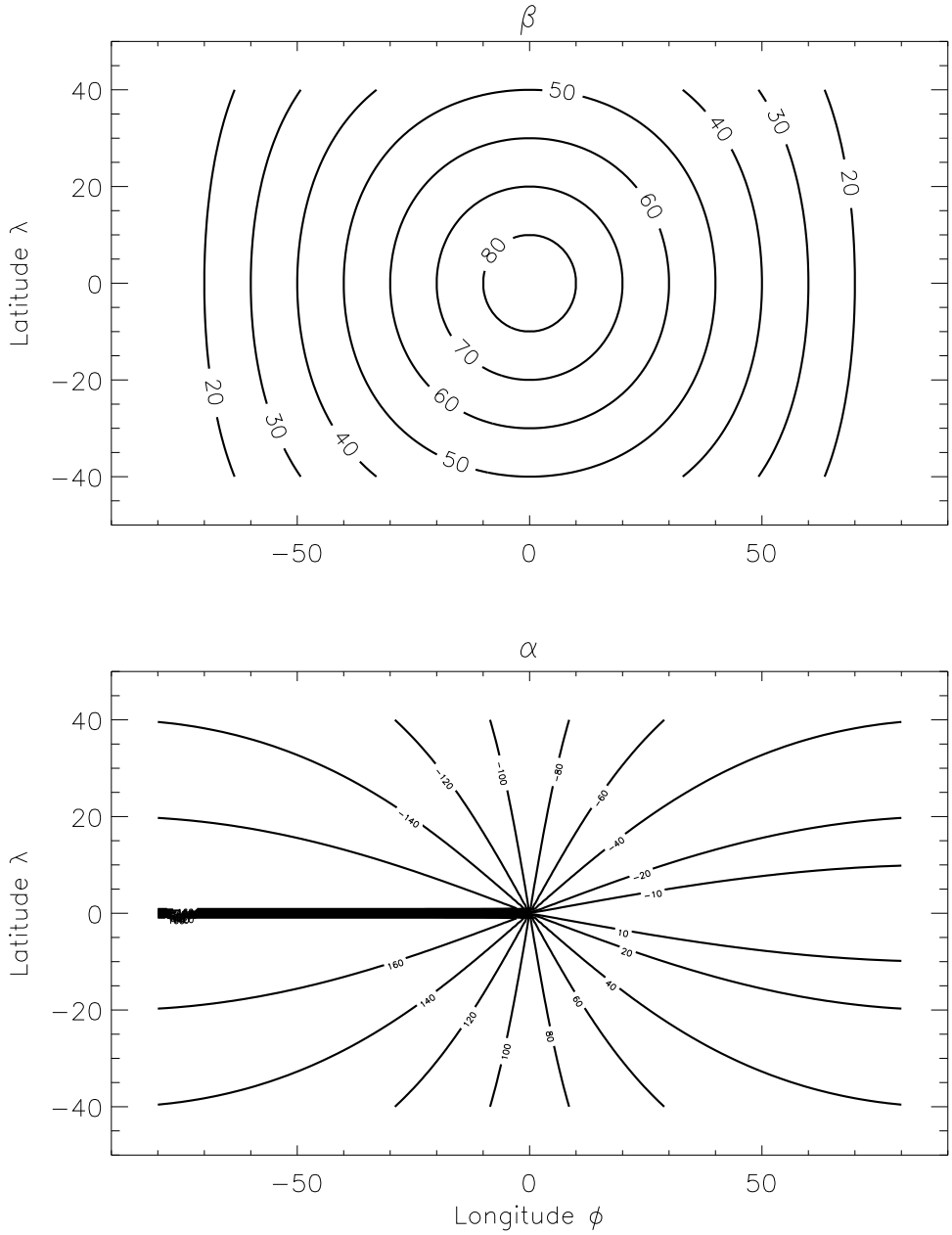

Figure 5. The transformation between (λ, ϕ) and (β, α), showing that any α value contains the information of both λ and ϕ.

4. Inversion solutions

4.1 By setting $\delta o = \delta + \triangle\delta$, the relationship between elliptic cone parameters and halo parameters can be derived by comparing Eqs. (4) and (5) with Eqs. (1) and (2)

$$R_c \cos\beta = D_{se} \tag{7}$$

$$R_c \tan\omega_y \sin\beta \sin\chi = SA_{xo} \cos\psi \sin \triangle\delta + SA_{yo} \sin\psi \cos\triangle\delta \tag{8}$$

$$-R_c \tan\omega_z \sin\beta \cos\chi = SA_{xo} \cos\psi \cos \triangle\delta - SA_{yo} \sin\psi \sin\triangle\delta \tag{9}$$

$$R_c \tan\omega_y \cos\chi = -SA_{xo} \sin\psi \sin \triangle\delta + SA_{yo} \cos\psi \cos\triangle\delta \tag{10}$$

$$R_c \tan\omega_z \sin\chi = -SA_{xo} \sin\psi \cos \triangle\delta - SA_{yo} \cos\psi \sin\triangle\delta \tag{11}$$

Eq. (7) shows that the distance between the solar disk center and the elliptic halo center, D_{se}, is determined by R_c and β, as shown in Figure 4. As CMEs propagate radially, R_c increases, and D_{se} increase too if the half of angular width ω_z is constant. This time-dependent $D_{se}$is valid for all cone-like models with the apex of cones located at the spherical center of the Sun. This characteristic may be used to distinguish the halo CMEs that are assumed to be formed by circular cone model with its apex located at the solar surface when the D_{se} is time-independent (Michalek et al., 2003).

4.2 By assuming that $\triangle\delta = \psi - \chi$, we have from Eq. (7) – (10)

$$(R_c \tan\omega_y \sin\beta + b) \tan\chi = d \tag{12}$$

$$-R_c \tan\omega_z \sin\beta - e \tan\chi = a \tag{13}$$

$$R_c \tan\omega_y - d \tan\chi = c \tag{14}$$

$$(R_c \tan\omega_z - c) \tan\chi = -d \tag{15}$$

$$a = SA_{xo} \cos^2\psi + SA_{yo} \sin^2\psi \tag{16}$$

$$b = SA_{xo} \cos^2\psi - SA_{yo} \sin^2\psi \tag{17}$$

$$c = -SA_{xo} sin^2\psi + SA_{yo} cos^2\psi \tag{18}$$

$$d = (SA_{xo} + SA_{yo})\sin\psi\cos\psi \tag{19}$$

$$e = (SA_{xo} - SA_{yo})\sin\psi\cos\psi \tag{20}$$

4.3 Using one-point and two-point observations to determine the propagation direction of CMEs

The number of halo parameters, SA_{xo}, SA_{yo}, D_{se}, α, ψ is less than the number of elliptic cone parameters, R_c, ω_y, ω_z, χ, β, $\alpha\dot{\mathrm{T}}$o obtain the unique solution of Eqs (6), (11) – (14) we need one more given parameter. As shown in Figure 5, the observed halo parameter α provides the information of both ϕ and λ. The following two ways can be used to invert the angle β and the unique solution of these equations.

• One-point observations

the location of the halo CME-associated flare or other near surface activity is the zero approximate of the CME propogation, i.e., the central axis of cones. Combining the information with the observed halo parameter α the first approximation of the central axis, λ and ϕ, and thus the elliptic cone parameter β can be determined from Figure 5.

• Two-point observations

Assuming that two spacecraft, such as the STEREO A and STEREO B, are located at the ecliptic plane, and the difference of their azimuthal angles is $\triangle\phi$. The central axis direction of a CME viewed from the STEREO A and STEREO B are (λ, ϕ_a) and (λ, $\phi_a + \triangle\phi$). The corresponding azimuthal angles relative to Yh (west) direction, α_a and α_b, can be observed by STEREO A and STEREO B, and can be used to calculate λ and ϕ_a as follows,

$$\begin{aligned} \cot\phi_a &= \frac{\tan\alpha_a}{\tan\alpha_b \sin\triangle\phi} - \cot\triangle\phi \\ \tan\lambda &= \tan\alpha_a \sin\phi_a \end{aligned} \tag{21}$$

4.4 The unique inversion solution of the elliptic cone model

• The unique determination of elliptic cone parameters R_c, χ, ω_y and ω_z in the case of

$\chi \neq 0$, which is valid for Type C of halo CMEs.

$$\begin{aligned} R_c &= D_{se}/\cos\beta \\ \tan\omega_y &= \frac{-(b-c\sin\beta)+[(b+c\sin\beta)^2+4\sin\beta d^2)]^{0.5}}{2R_c\sin\beta} \\ \tan\chi &= (R_c\tan\omega_y - c)/d \\ \tan\omega_z &= (a + e\tan\chi)/R_c\sin\beta \end{aligned} \tag{22}$$

• The unique solution for elliptic cone parameters R_c, ω_y and ω_z in the case of $\chi = 0$, which is valid for Types A and B of halo CMEs.

$$\begin{aligned} R_c &= D_{se}/\cos\beta \\ \tan\omega_z &= SA_{xo}/(R_c\sin\beta) \\ \tan\omega_y &= SA_{yo}/R_c \end{aligned} \tag{23}$$

• The unique solution for the circular cone model, i.e., when $\chi = 0$ and $\omega_y = \omega_z$. In this case, the angle β can be determined simply using halo images alone. The solution is the same as Xie et al. (2004) and valid only for a small part of Type A, i.e., when $\omega_y = \omega_z$.

$$\begin{aligned} \sin\beta &= SA_{xo}/SA_{yo} \\ R_c &= D_{se}/\cos\beta \\ \tan\omega &= SA_{yo}/R_c \end{aligned} \tag{24}$$

5. Prediction and inversion

Using Eqs. (3) – (6) and the values of 6 elliptic cone parameters λ, ϕ, ω_y, ω_z, R_c and χ, we can predict the corresponding ellipse projected onto the plane of the sky Y_hZ_h, and obtaine the 5 halo parameters SA_{xo}, SA_{yo}, D_{se}, ψ, and α that are expected to be observed. Figures 6 and 7 display the given base of a cone in the $X_eY_eZ_e$ and $X_cY_cZ_c$ coordinate systems and the predicted three halos in the $X_hY_hZ_h$ coordinate system for the cases of $\chi = 0°$ and $\chi = -30°$, respectively. The left panels show the values of 6 elliptic cone parameters used in the prediction, and right panels show predicted halos and the 5 halo parameters supposed to be observed by spacecraft, such as STEREO A, SOHO, and STEREO B.

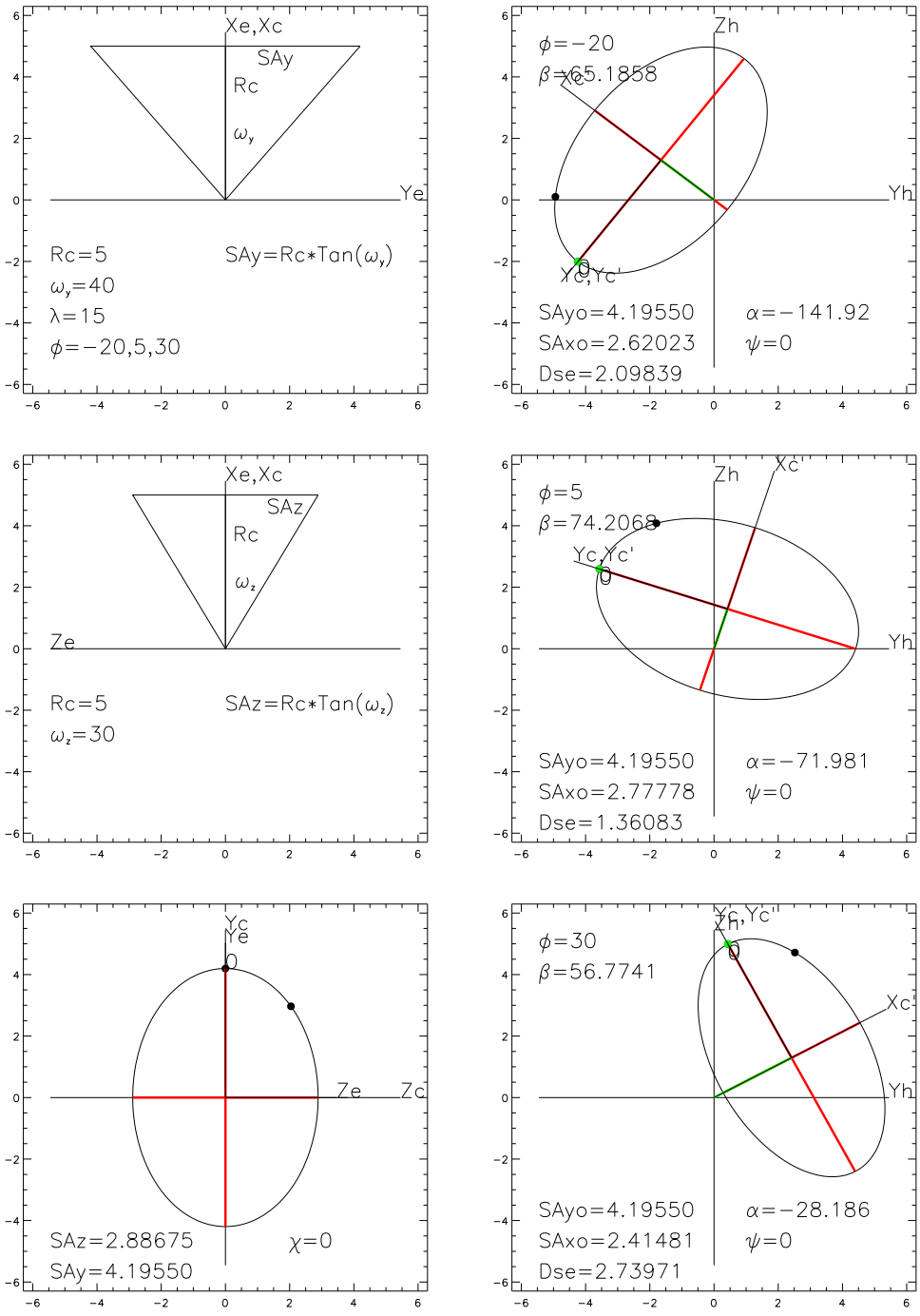

Figure 6. The prediction of halos with $\chi = 0$ and three $\phi = -20°, 5°, 30°$. The predicted halos are supposed to be observed by STEREO A, SOHO, and STEREO B

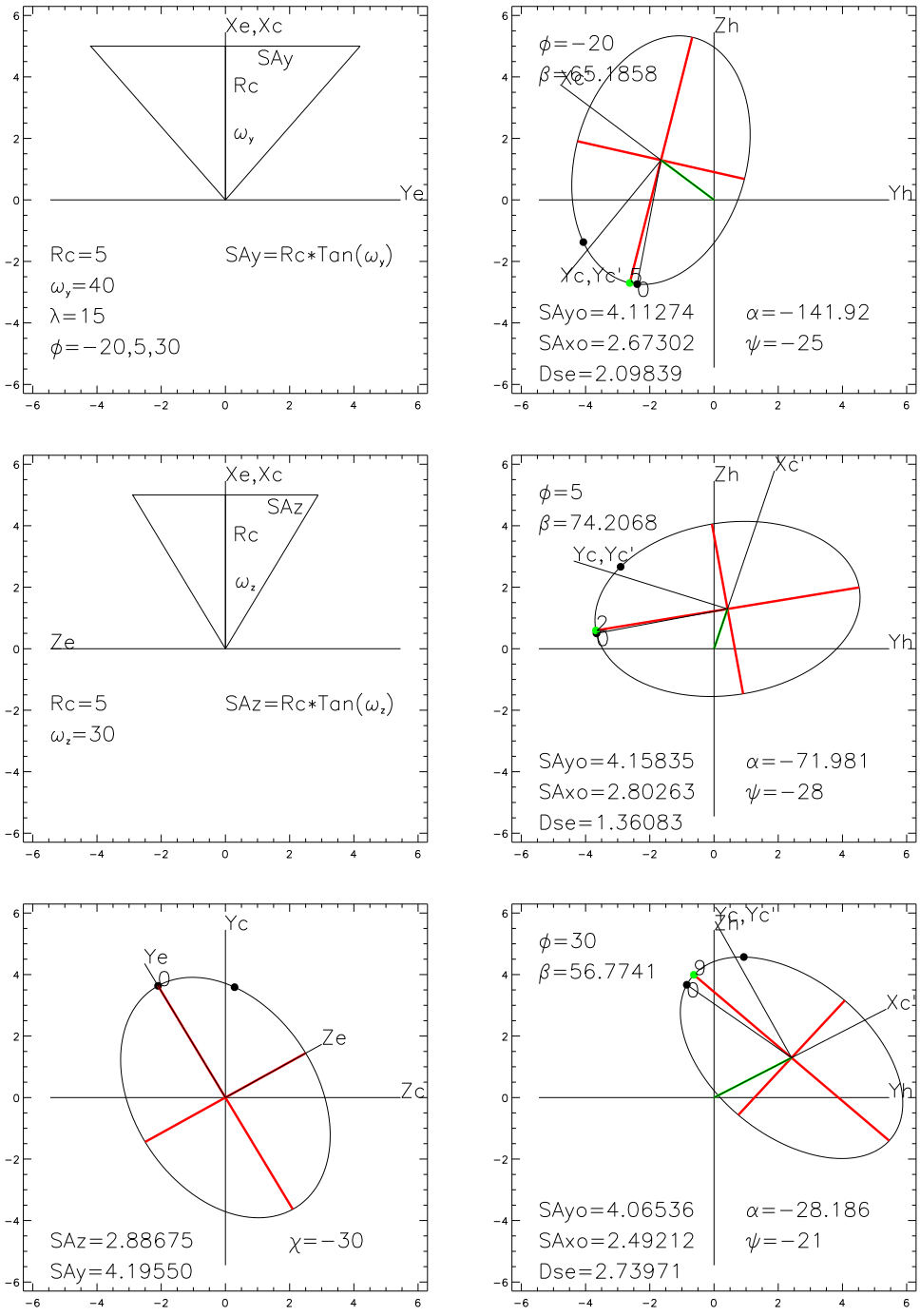

Figure 7. The prediction of halos with $\chi = -300$ and three $\phi = -20°, 5°, 30°$. The predicted halos are supposed to be observed by STEREO A, SOHO, and STEREO B.

Substituting $\triangle\phi$, α_a and α_b in Eq. (21) with the azimuthal difference between two spacecraft and the two calculated α angles that supposed to be observed, the longitude ϕ_a, and latitude λ of the CME propagation can be calculated, and the latitude β_a of the CME propagation can be determined using Eq. (3).

Based on the given D_{se} and the obtained β_a, the parameter R_c can be calculated using Eq. (7). Finally using the predicted values of halo parameters ψ, SA_{xo}, SA_{yo} for $\chi = 0$ and $\chi = -30$ (see Figures 6 and 7), and corresponding Eq. (23) and (22), the elliptic cone parameters ω_y, ω_z, and χ can be obtained. Table 1 shows the original (the second column of Table 1) and inverted (the third column) values of elliptic cone parameters λ, ϕ, R_c, ω_y, ω_z, and χ. It indicates that the inverted values of λ, ϕ, R_c ω_y, $\omega_z$for both $\chi = 0$ and $\chi = -30$ are nearly identical with the original ones, suggesting that the propagation direction, speed and angular widths can be accurately inverted using the two-point observations and the algorithm developed here. For the case of $\chi \neq 0$, the inverted parameter χ slightly differs from the original one.

It is not easy to distinguish Type A halos formed by elliptic cones with $\omega_y > \omega_z$, and $\chi = 0$ from that formed by circular cones, and is often wrongly replacing the halo parameters SA_{xo}, SA_{yo}, D_{se} and α from Type A halo CMEs into Eqs. (24) valid for the circular cone model to determine the circular cone parameters β, R_c, and ω_z. The last column shows the result obtained using halo parameters from Figure 6. All inverted parameters are significantly different from the original ones.

Table 1. The inverted elliptic cone parameters

Parameters	Original values	Inverted	values	
		$\chi = 0$	χ = -30	Circular
λ	15	15.0014	15.0014	28.7958
ϕ	-20	-19.9979	-19.9979	-44.5483
β	65.1856	65.1856	65.1856	38.6479
R_c	5	4.99997	4.99997	2.68681
ω_y	40	40.0002	39.9302	57.3644
ω_z	30	30.0002	30.3534	57.3644
χ	0.0, -30	0.0	-26.2962	

6. Summary and Discussions

• We have shown that the direction from the solar disk center to the center of elliptic halos, D_{se}, is the projection of the central axis of 3-D cones (or CME propagation direction) onto the plane of the sky. Based on the direction of semi-minor or semi-major axis of elliptic halos relative to D_{se}, elliptic halo CMEs can be classified into three types. For type A halo CMEs their semi-minor axes are aligned with D_{se}; For type B, it is semi-major axes that are aligned with D_{se}; For type C, both semi-axes are not aligned with D_{se}.

• The elliptic cone model can be used to produce all the three types of halo CMEs if all six elliptic cone parameters are given. The elliptic cone models with $\chi = 0$ may produce Type A when $\omega_y > \omega_z$ and Type B when $\omega_y < \omega_z$. The elliptic model with $\chi \neq 0$ may produce Type C halo CMEs.

• The direction of Y_c' or Y_c that is perpendicular to the direction of D_{se}, may be used to define the orientation both for the observed 2-D elliptic halo CMEs and the supposed elliptic base of 3-D cones. This reference direction can be used to derive the equations that relate the elliptic cone parameters to the halo parameters, and the equations can be used to invert the elliptic cone parameters from the halo parameters.

• Five halo parameters cannot be used to uniquely determine six elliptic cone parameters. One more halo parameter is needed. The angle α is not only a halo parameter but also a elliptic cone parameter. Eq. (3) and Figure 5 show that angle α is determined by both ϕ and λ, and contains the information of both ϕ and λ that characterize the CME propogation direction. Two ways, i.e., using one-point and two-point observations, are presented in Section 4 to determine the β. The unique inversion solution for elliptic cone model can thus be obtained.

• The elliptic halo CMEs observed by multi-spacecraft, such as STEREO A,

SOHO, and STEREO B, have been predicted given the elliptic cone parameters and the location of three spacecraft (see Figures 6 and 7). The validity of the elliptic cone model may be critically examined by comparing predicted halo CMEs with multi-spacecraft observation of halo CMEs.

• Replacing the values of halo parameters in Figures 6 and 7, that are predicted on the basis of the given elliptic cone parameters, into the inversion equations (21) – (24), the inverted elliptic cone parameters are listed in Table 1. It shows the CME propagation direction and speed can be accurately inverted using the two-point method presented here for all three types of halo CMEs. For Types A and B halo CMEs, all elliptic cone parameters can be accurately inverted using the two-point method. Because the elliptic cone model becomes the circular cone model when $\chi = 0$ and $\omega_y = \omega_z$, the method is certainly good for Type A halo CMEs formed by circular cone model. As shown by the rightest column of Table 1, however, unless a Type A halo CME can be determined to be formed by the circular cone shell of CME plasma, the circular cone model should not be used to invert the solution for Type A halo CMEs.

• Michalek et al. (2003) presented a different circular cone model for inverting halo CMEs. The apex of the circular cone was assumed to be located on the solar surface, instead of at the spheric center of the Sun, and the distance of the center of elliptic halos from the solar disk center, D_{se} is thus time-independent, instead of time-dependent as shown by Eq. (7). To invet the circular cone parameters using the model, it is necessary to first check whether or not the parameter $D_{se}$of the halo CME is constant.

• There are halo CMEs that are not purely elliptic. Some of them may be caused by ice-cream cone models (Zhao, 2005).

• The accuracy of inversion solutions depends significantly on the halo parameters

from observed halo CMEs. To further improve the inversion solution it is necessary to develop techniques for rather objectively measuring the halo parameters from white-light images.